

## Investigation of discrete $\gamma$ radiation in interactions of 14.9-MeV neutrons with natural silicon by a total $\gamma$ -radiation measurement technique

Hong-Yu Zhou,<sup>1,\*</sup> Fu-Guo Deng,<sup>2</sup> Qiang Zhao,<sup>3</sup> Jun Su,<sup>1</sup> Bao-Kui Zhao,<sup>1</sup> Li-Ming Dong,<sup>1</sup>  
Guo-Ying Fan,<sup>1</sup> and Feng-Shou Zhang<sup>1</sup>

<sup>1</sup>Key Laboratory of Beam Technology and Material Modification of Ministry of Education,  
Institute of Low Energy Nuclear Physics, Beijing Normal University, Beijing 100875, China

<sup>2</sup>Department of Physics, Beijing Normal University, Beijing 100875, China

<sup>3</sup>School of Nuclear Science and Engineering, North China Electric Power University, Beijing 102206, China

(Received 17 July 2010; revised manuscript received 24 August 2010; published 21 October 2010)

The discrete  $\gamma$  radiation in the interaction of 14.9-MeV neutrons and a natural silicon sample is investigated with a total  $\gamma$ -radiation measurement (TGRM) technique. Fifty prompt  $\gamma$  lines, one delayed  $\gamma$  line, and seven final nuclei are identified. Forty-one possible transitions are designated. Differential production cross sections of 40  $\gamma$  lines at 40°, 55°, 90°, 125°, and 140° are determined. Using relative differential production cross sections, accurate integral isotopic cross sections of the  $^{28}\text{Si}(n,p)^{28}\text{Al}$  reaction are determined, and partial integral isotopic cross sections of the  $^{28}\text{Si}(n,n')^{28}\text{Si}$ ,  $^{28}\text{Si}(n,\alpha)^{25}\text{Mg}$ ,  $^{29}\text{Si}(n,n')^{29}\text{Si}$ , and  $^{30}\text{Si}(n,n')^{30}\text{Si}$  reaction channels are also estimated. The present results are in good agreement with some recent experimental and evaluated results.

DOI: 10.1103/PhysRevC.82.047602

PACS number(s): 28.20.-v, 25.40.Fq, 29.87.+g

Natural silicon has important applications in many new technology fields, such as nuclear detectors, semiconductor integrated circuits, solar energy, and fusion energy. Especially, the investigation by Peit *et al.* [1] showed that Si and its composites with C (SiC) can offer structural materials with low radioactivity and afterheat and high operating temperatures for fusion reactors. Therefore, accurate knowledge of the behavior of natural silicon in a 14-MeV neutron irradiation field is very important for the development of fusion energy technology, such as production probabilities of  $\gamma$  rays, neutrons, protons, and  $\alpha$  particles from  $\text{Si}(n,x\gamma)$  reactions and hardening, embrittlement, and creep of Si material induced by fast neutron irradiation. However, existing experimental results for the  $\text{Si}(n,x\gamma)$  reaction induced by 14-MeV neutrons [2–16] still suffer from some defects. For example, the number of identified  $\gamma$  lines is lower, data accuracy is very poor (in general, >10%), and the discrepancy between different data groups is very large. At the end of the last century we established a pulsed-beam, fast neutron, time-of-flight (TOF) spectrometer and developed a total  $\gamma$ -radiation measurement (TGRM) technique used in  $(n,x\gamma)$  experiments at the neutron physics laboratory at Beijing Normal University [17,18]. TGRM combines the usual measurement technique of prompt  $\gamma$  radiation with the lifetime correction method of delayed  $\gamma$  radiation, so that it can quantitatively determine  $\gamma$ -radiation yields not only for a prompt component but also for a delayed component in a TOF experiment simultaneously. In this work, we report some new results on the investigation of discrete  $\gamma$  radiation in the interaction of 14.9-MeV neutrons with a natural silicon obtained by the TGRM technique.

The experiment was carried out in a pulsed Cockcroft-Walton accelerator. The sample is a cylindrical crystal silicon  $3.0 \times 3.0$  cm in diameter and weighing 50.52 g. The repetition

frequency of the pulsed deuteron beam is 3.2 MHz. Neutrons incident on the sample are produced from the  $\text{T}(d,n)^4\text{He}$  reaction. The neutron energy in the 0° direction with respect to the deuteron beam is  $14.9 \pm 0.5$  MeV, and the average intensity is  $\sim 5 \times 10^8$  n/s in  $4\pi$  sr. The neutron flux incident on the sample is determined by the counts of the associated particles of  $^4\text{He}$ , which are measured by an Au-Si detector. Absolute  $\gamma$ -ray yields are measured by a coaxial Ge(Li) detector. The TOF technique is employed to reduce the background caused by the primary and scattered neutrons. Two time gates, 30 and 160 ns, which cover the time regions containing total prompt radiation and partial delayed radiation, respectively, are set to record the total  $\gamma$ -ray spectrum (containing total prompt and partial delayed  $\gamma$  radiation) and the pure delayed  $\gamma$ -ray spectrum, respectively. Measurements are made at 40°, 55°, 90°, 125°, and 140° relative to the incident neutron direction. The elemental differential production cross section of a discrete  $\gamma$  ray with energy  $E_\gamma$  at angle  $\theta$  with respect to the incident neutron direction can be calculated by the following formula:

$$\frac{d\sigma}{d\Omega}(E_\gamma, \theta) = \frac{N_\gamma(E_\gamma, \theta)}{4\pi\phi_n N \varepsilon(E_\gamma)} f, \quad (1)$$

where  $\phi_n$  is the number of neutrons incident on the sample.  $N_\gamma(E_\gamma, \theta)$  is the yield of  $\gamma$  radiation with energy  $E_\gamma$  detected in the  $\theta$  direction. For a pure prompt  $\gamma$  line, it is the net count in the full-energy peak. For pure delayed  $\gamma$  radiation and mixed  $\gamma$  radiation, it can be calculated by the lifetime correction method [17].  $\varepsilon(E_\gamma)$  is the absolute detection efficiency of the full-energy peak by the Ge(Li) detector for a  $\gamma$  ray with energy  $E_\gamma$ .  $N$  is the number of atoms per unit area of the sample in the incident neutron direction.  $f$  is the correction factor to neutron flux and  $\gamma$ -ray yields. Details of the experiment and data analysis are the same as for measurements of aluminum samples [18].

Figures 1 and 2 show the total and the delayed  $\gamma$ -radiation energy spectra, respectively, after subtraction of the respective

\* zhy@bnu.edu.cn

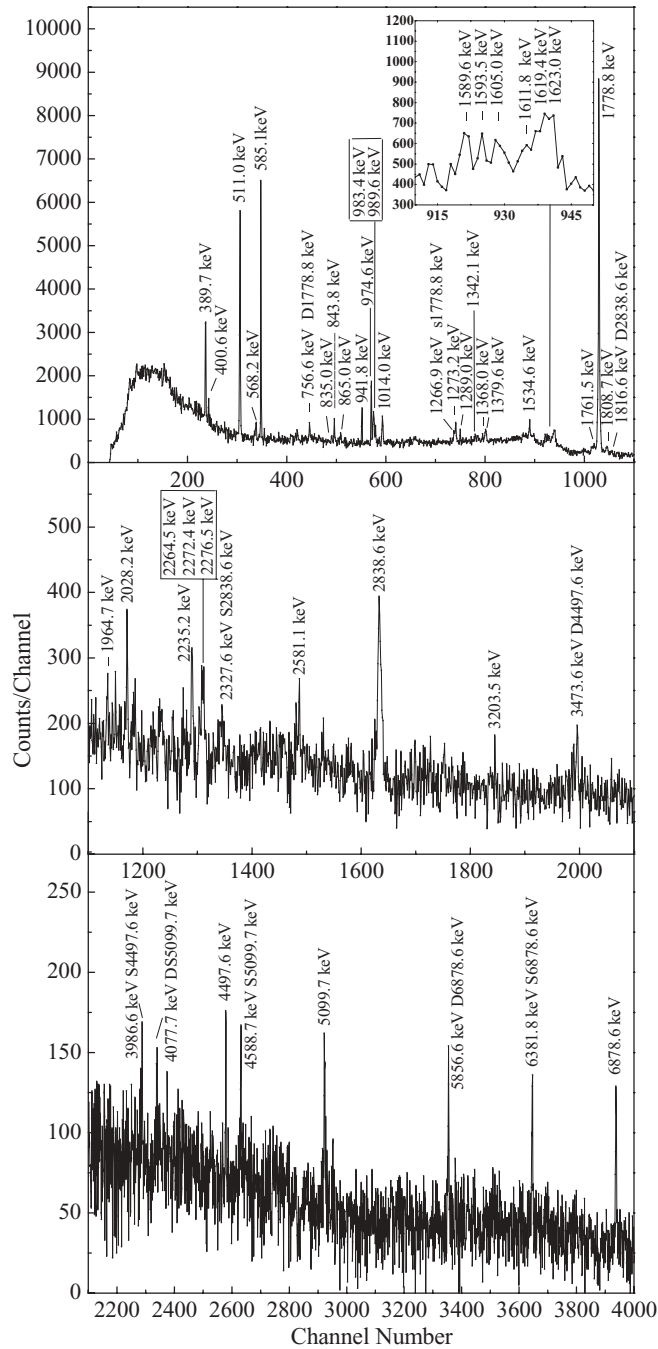


FIG. 1. Total  $\gamma$ -ray spectrum for the interaction of 14.9-MeV neutrons with natural silicon ( $\theta = 90^\circ$ ).

background spectra without sample at  $90^\circ$ . According to the systematic knowledge of 14.9-MeV neutron-induced  $^{28,29,30}\text{Si}(n,\gamma)$  reactions, 50 prompt  $\gamma$  lines, 1 delayed  $\gamma$  line, and 7 final nuclei are identified. Forty-one possible transitions are designated. The elemental differential production cross sections of 40  $\gamma$  lines at  $40^\circ$ ,  $55^\circ$ ,  $90^\circ$ ,  $125^\circ$ , and  $140^\circ$  are determined. The 511-keV line comes from the annihilation radiation background in Figs. 1 and 2. The 139.7-keV line comes from  $^{75m}\text{Ge}$  in the Ge(Li) detector material, and the 197.1-keV line comes from  $^{19m}\text{F}$  in the surrounding materials; only the 1778.8-keV line is delayed  $\gamma$  radiation

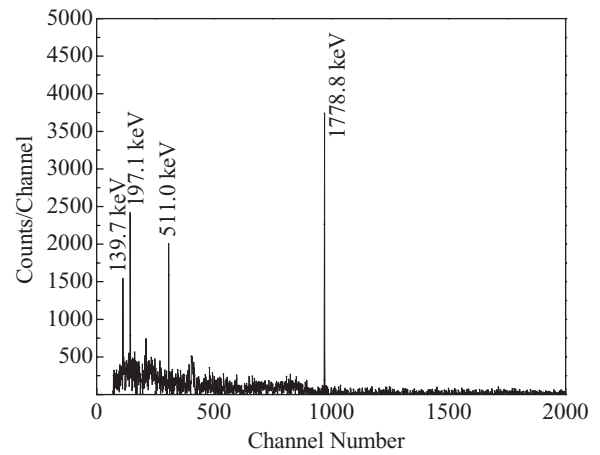


FIG. 2. Delayed  $\gamma$ -ray spectrum for the interaction of 14.9-MeV neutrons with natural silicon.

coming directly from the natural silicon sample in Fig. 2. The preceding partial results are listed in Table I. To shorten this report, of the elemental differential production cross sections at five angles, only those at  $90^\circ$  are listed in Table I. Many of the data at other angles will be given in another report. In Table I, DEP and SEP represent double and single escape peaks, respectively. We found 10 escape peaks in similar investigations for the first time.

In Table I,  $1778.8^p$  and  $1778.8^d$  represent the prompt and the delayed 1778.8-keV lines that are produced from  $^{28}\text{Si}(n,n'\gamma)^{28}\text{Si}^*$  and  $^{28}\text{Si}(n,p)^{28}\text{Al}(\beta^-)^{28}\text{Si}^*(\gamma)$  ( $f_{1/2} = 2.24$  m) processes, respectively. Figure 3 shows the angular distributions of the isotopic differential production cross sections for the three components of 1778.8-keV lines; Figs. 3(A), 3(B), and 3(C) show the angular distributions of the prompt + delayed, prompt, and delayed components, respectively. The respective Legendre polynomial fitting curves were obtained from the present experimental data, and their coefficients are shown in Fig. 3. Some previous experimental data [2,5,6] are also shown in Fig. 3 for comparison.

Using the relative differential production cross sections, the accurate integral isotopic cross sections of the  $^{28}\text{Si}(n,p)^{28}\text{Al}$  reaction are determined, and the partial integral isotopic cross sections of the  $^{28}\text{Si}(n,n')^{28}\text{Si}$ ,  $^{28}\text{Si}(n,\alpha)^{25}\text{Mg}$ ,  $^{29}\text{Si}(n,n')^{29}\text{Si}$ , and  $^{30}\text{Si}(n,n')^{30}\text{Si}$  reaction channels are also estimated (see Table II). In general, the integral reaction cross sections obtained by the  $\gamma$ -production cross sections can only be regarded as estimates and references for the actual reaction cross sections because the integral cross section of a reaction channel is obtained by summing the corresponding differential  $\gamma$ -production cross sections for ground-state  $\gamma$  transitions. In general, this integral reaction cross section is smaller than the actual reaction cross section, for many reasons [19]. For example, for some reactions with a high threshold, close to 14 MeV, the partial residual nuclei are possibly in the ground state, so that no discrete  $\gamma$  ray is observed. For example, the threshold energies of the  $^{28}\text{Si}[(n,np) + (n,d)]^{27}\text{Al}$  reaction are 12.0 and 9.69 MeV, respectively, and both theoretical and experimental investigations show that for the 14-MeV neutron-induced  $^{28}\text{Si}[(n,np) + (n,d)]^{27}\text{Al}$  reaction, the probability

TABLE I. Differential production cross section of the total  $\gamma$  radiation from interactions of 14.9-MeV neutrons with a natural silicon sample.

$E_\gamma$ (keV)	Final nucleus	Transition (keV)	Cross section (mb/sr, 90°)
389.7	$^{25}\text{Mg}$	974.8 to 585.1	$1.54 \pm 0.10$
400.6	$^{28}\text{Al}$	1372.8 to 972.2	$0.30 \pm 0.05$
568.2			$0.44 \pm 0.05$
585.1	$^{25}\text{Mg}$	585.1 to 0	$3.43 \pm 0.19$
756.6	$^{28}\text{Si}$	DEP of 1778.8	
835.0	$^{25}\text{Mg}$	2801.1 to 1964.6	$0.21 \pm 0.05$
843.8	$^{27}\text{Al}$	843.8 to 0	$0.65 \pm 0.06$
865.0	$^{28}\text{Al}$	2485.0 to 1620.1	$0.33 \pm 0.06$
941.4	$^{28}\text{Al}$	972.2 to 30.6	$0.77 \pm 0.07$
974.6	$^{25}\text{Mg}$	974.8 to 0	$2.13 \pm 0.13$
983.4	$^{28}\text{Al}$	1014.0 to 30.6	$1.56 \pm 0.09$
989.7	$^{25}\text{Mg}$	1964.6 to 974.8	$0.55 \pm 0.14$
1014.0*	$^{28}\text{Al}$	1013.6 to 0	$1.32 \pm 0.15$
	$^{27}\text{Al}$	1014.5 to 0	
1266.9	$^{28}\text{Si}$	SEP of 1778.8	
1273.2	$^{29}\text{Si}$	1273.2 to 0	$0.71 \pm 0.11$
1289.0	$^{28}\text{Si}$	9702.0 to 8413.3	$0.48 \pm 0.12$
1342.1	$^{28}\text{Al}$	1372.8 to 30.6	$0.45 \pm 0.09$
1368.0	$^{27}\text{Al}$	2210.0 to 843.8	$0.37 \pm 0.07$
1379.6	$^{25}\text{Mg}$	1964.6 to 585.1	$0.81 \pm 0.10$
1534.6	$^{28}\text{Si}$	8413.3 to 6878.6	$0.78 \pm 0.19$
1589.6	$^{28}\text{Al}$	1620.1 to 30.6	$0.57 \pm 0.10$
1595.7	$^{28}\text{Si}$	11 298 to 9702.0	$0.60 \pm 0.10$
1605.1	$^{28}\text{Al}$	3876.0 to 2272.0	$0.62 \pm 0.09$
1611.8	$^{25}\text{Mg}$	1611.7 to 0	$0.86 \pm 0.10$
1618.8	$^{28}\text{Al}$	1620.1 to 0	$0.89 \pm 0.13$
1623.4	$^{28}\text{Al}$	1622.7 to 0	$1.16 \pm 0.11$
1761.5	$^{25}\text{Mg}$	2736.0 to 974.8	$0.57 \pm 0.10$
1778.8 <sup>p</sup>	$^{28}\text{Si}$	1778.8 to 0	$24.3 \pm 1.0$
1778.8 <sup>d</sup>	$^{28}\text{Si}$	1778.0 to 0	$16.9 \pm 0.7$
1808.7	$^{26}\text{Mg}$	1808.7 to 0	$0.35 \pm 0.10$
1816.6	$^{28}\text{Si}$	DEP of 2836.5	
1964.7*	$^{28}\text{Si}$	11445 to 9479.5	$0.39 \pm 0.10$
	$^{25}\text{Mg}$	1964.6 to 0	
2028.2	$^{29}\text{Si}$	2028.2 to 0	$0.54 \pm 0.09$
2235.4	$^{30}\text{Si}$	2235.5 to 0	$0.90 \pm 0.09$
2265.8	$^{28}\text{Al}$	4846.0 to 2582.0	$0.49 \pm 0.11$
2272.4	$^{28}\text{Al}$	2272.0 to 0	$0.69 \pm 0.10$
2277.5	$^{25}\text{Mg}$	5012.0 to 2736.0	$0.47 \pm 0.10$
2327.6	$^{28}\text{Si}$	SEP of 2836.5	
2581.1	$^{28}\text{Al}$	2581.0 to 0	$0.93 \pm 0.30$
2838.6	$^{28}\text{Si}$	4617.8 to 1778.8	$3.94 \pm 0.46$
3203.5	$^{28}\text{Si}$	9480.0 to 6276.5	$0.93 \pm 0.19$
3473.6	$^{28}\text{Si}$	DEP of 4497.6	
3986.6	$^{28}\text{Si}$	SEP of 4497.6	
4077.7	$^{28}\text{Si}$	DEP of 5099.7	
4497.6	$^{28}\text{Si}$	6276.5 to 1778.8	$1.04 \pm 0.20$
4588.7	$^{28}\text{Si}$	SEP of 5099.7	
5099.7	$^{28}\text{Si}$	6878.6 to 1778.8	$1.87 \pm 0.41$
5856.6	$^{28}\text{Si}$	DEP of 6878.6	
6381.8	$^{28}\text{Si}$	SEP of 6878.6	
6878.6	$^{28}\text{Si}$	6878.6 to 0	$2.19 \pm 0.37$

populated in the ground state of the residual  $^{27}\text{Al}$  is much higher than the one populated in the excited state of  $^{27}\text{Al}^*$  [11]. Therefore, the integral cross section obtained by summing the

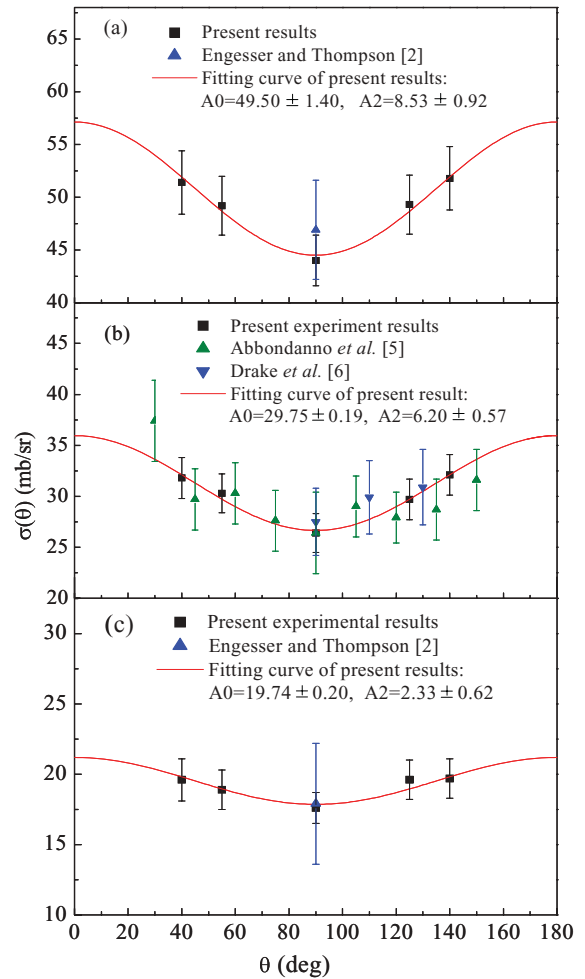


FIG. 3. (Color online) Angular distribution of the differential isotopic production cross section of 1778.8-keV  $\gamma$  rays produced in 14.9-MeV neutron-induced  $^{28}\text{Si}(n,xy)^{28}\text{Al}$  reactions. Angular distribution of production cross sections of (a) the prompt + delayed components, (b) the prompt component, and (c) the delayed component in 1778.8-keV  $\gamma$  rays.

differential production cross sections of the  $\gamma$  lines transiting to the ground state of  $^{27}\text{Al}$  (24.5 mb) is much smaller than the actual integral cross section ( $\sim 160$  mb). That is, this cross section can, in general, be considered an estimation of the minimum value of the actual reaction cross section. The integral cross section of the  $^{28}\text{Si}(n,p)^{28}\text{Al}$  reaction obtained with the foregoing method is  $111 \pm 10$  mb, which is much smaller than the recent evaluation value (248 mb) [20]. However, there is a method with which the precise cross section of the  $^{28}\text{Si}(n,p)^{28}\text{Al}$  reaction can be obtained.  $^{28}\text{Al}$  is a nucleus with  $\beta^-$  decay ( $f_{1/2} = 2.24$  m), the ground state of which reaches the first excited state of  $^{28}\text{Si}$  (1778.8 keV) through  $\beta^-$  decay with a 100% branching ratio, and the first excited state of  $^{28}\text{Si}$  transits to the ground state of  $^{28}\text{Si}$  through 1778.8-keV  $\gamma$  radiation with a 100% branching ratio, so that only the delayed 1778.8-keV  $\gamma$  radiation ( $f_{1/2} = 2.24$  m) can contain the complete  $^{28}\text{Si}(n,p)^{28}\text{Al}$  reaction process and completely avoid total uncertainty. Therefore, the accurate integral cross section of the  $^{28}\text{Si}(n,p)^{28}\text{Al}$  reaction channel can be obtained

from the angular distribution of the differential production cross section of the delayed 1778.8-keV  $\gamma$  radiation. The result for the  $^{28}\text{Si}(n,p)^{28}\text{Al}$  reaction listed in Table II ( $248.0 \pm 2.5$  mb) was determined by means of this method, which is in precise agreement with the recent estimated value (248 mb) [20].

Analyzing the foregoing results leads us to several conclusions. First, compared to the earlier results reported by other laboratories [2–16], the present work provides much richer information on 14-MeV neutron-induced  $^{28}\text{Si}(n,x\gamma)$  reactions. In the present work, 50  $\gamma$  lines are identified and the differential production cross sections of 40  $\gamma$  lines are determined, which is about three times more than the number identified in all previous work. In addition, the present work provides complete angular distribution data at five angles for the 40  $\gamma$  lines observed and the reaction cross section data for the eight reaction channels. Second, the present data accuracy is greatly increased compared to that of earlier experimental results [2–16]. This is especially true for the data accuracy of the several characteristic  $\gamma$  lines with substantial radiation yields, such as 585.1, 1778.8, and 2838.6 keV. Here the accuracies reach 3%–5%. Even the accuracy of the activation cross section reaches 1%. Third, the present results are in good agreement with the results of Engesser and Thompson [2], Abbondanno *et al.* [5], Drake *et al.* [6], Grenier *et al.* [8], and Buchanan *et al.* [9], although there are larger differences in the experimental conditions and methods. Finally, it can be seen from Table II that for the integral cross sections of the

TABLE II. Integral isotopic cross sections of some reactions of 14.9-MeV neutrons with natural silicon.

Reaction	Integral isotopic cross section (mb)	
	This work	Calculated value [20]
$^{28}\text{Si}(n,p)^{28}\text{Al}$	$248.0 \pm 2.5$	248
$^{28}\text{Si}(n,n')^{28}\text{Si}$	$405 \pm 18.0$	460
$^{28}\text{Si}(n,\alpha)^{25}\text{Mg}$	$93.0 \pm 5.0$	165
$^{28}\text{Si}[(n,np) + (n,d)]^{27}\text{Al}$	$26.0 \pm 3.0$	160
$^{29}\text{Si}(n,n')^{29}\text{Si}$	$309.0 \pm 31.0$	460
$^{29}\text{Si}(n,\alpha)^{26}\text{Mg}$	$129.0 \pm 13.0$	130
$^{30}\text{Si}(n,n')^{30}\text{Si}$	$372.0 \pm 37.0$	471

$^{28}\text{Si}(n,p)^{28}\text{Al}$  reaction, the present result ( $248.0 \pm 2.5$  mb) is in precise agreement with the recent estimated value (248 mb) [20]. This shows that the TGRM technique combining both the prompt and the delayed  $\gamma$ -radiation yield measurements is very reliable.

The authors are grateful to C. Wen, L. Lan, H. Yang, and W. Zhou for participating in the experiment. This project was supported by the National Natural Science Foundation of China under Grant No. 11025524, the National Basic Research Program of China under Grant No. 2010CB832903, and the Doctoral Station Foundation of Ministry of Education of China under Grant No. 200800270017.

- [1] S. J. Peit, E. T. Cheng, and L. J. Porter, *Fusion Technol.* **17**, 636 (1990).
- [2] F. C. Engesser and W. E. Thompson, *J. Nucl. Energy* **21**, 487 (1967).
- [3] M. D. Goldberg, M. V. May, and J. R. Stehn, *Brookhaven National Laboratory Report BNL 400*, 2nd ed. (Brookhaven National Laboratory, Upton, NY, 1962).
- [4] Z. R. Shi *et al.*, *Chin. J. Nucl. Phys.* **1**, 45 (1979).
- [5] U. Abbondanno *et al.*, *J. Nucl. Energy* **27**, 227 (1973).
- [6] D. M. Drake, E. D. Arthur, and M. G. Silbert, *Nucl. Sci. Eng.* **65**, 49 (1978).
- [7] J. T. Prud'Homme *et al.*, *Tex. Nucl. Corp. Rep. Afswc-Tr-60-30* (Texas Nuclear Corp., Houston, 1960).
- [8] G. Grenier, B. Duchemin, and D. Parisot, *Exp. Rep. CEA R-4634* (Commissariat A L'Energie Atomique, Saclay, France, 1974).
- [9] P. S. Buchanan, D. O. Nellis, and W. E. Tucker, *Rep. Oro-2791-32* (Nuclear-Chicago Corp., Chicago, IL, 1971).
- [10] K. A. Connell and A. J. Cox, *Int. J. Appl. Radiat. Isotopes* **26**, 71 (1975).
- [11] S. Hlavac *et al.*, *Proceedings, International Conference on Nuclear Data for Science and Technology* (Bologna, Italy, 1997), p. 393.
- [12] I. Murata, J. Yamamoto, and A. Takahashi, *Proceedings, International Conference on Nuclear Data for Science and Technology* (Mito, Japan, 1988), p. 275.
- [13] P. W. Martin and D. T. Stewart, *Can. J. Phys.* **46**, 1657 (1968).
- [14] B. A. Benetsky, I. M. Frank, and C. R. Du, *Congres International De Physique Nucleaire* (CNRS, Paris, 1964), p. 817.
- [15] B. A. Benetsky, Yu. P. Betin, and Ya. Gonzatko, *Sov. Phys. JETP* **18**, 640 (1964).
- [16] V. M. Bezotosnyj *et al.*, *Proceedings, 5th All Union Conference on Neutron Physics* (Kiev, USSR, September, 1980), Vol. 2, p. 21.
- [17] H. Y. Zhou, G. S. Huang, and G. Y. Fan, *Nucl. Instrum. Methods A* **371**, 504 (1996).
- [18] H. Y. Zhou and G. S. Huang, *Nucl. Sci. Eng.* **125**, 61 (1997).
- [19] H. Y. Zhou, F. G. Deng, X. J. Ding *et al.*, *Nucl. Sci. Eng.* **157**, 354 (2007).
- [20] A. J. Koning, M. B. Chadwick, and P. G. Young, *ENDF/VI, Module 4: Evaluation* (Los Alamos National Laboratory, Los Alamos, NM, 1998).